Fusion Algorithm For Color Microbiological Organisms Images In Automatized Microscopes

Josué Álvarez-Borrego*[a], Mario Alonso Bueno-Ibarra[a], Vitaly Kober[b], Cristian Gallardo-Escárate[a],
Maria C. Chávez-Sánchez[c], Emma Fájer-Ávila[c]
CICESE, [a]Dirección de Telemática, [b]Departamento de Ciencias de la Computación, Km. 107
Carretera Tijuana-Ensenada, Ensenada, B. C., México. C.P. 22860
[c]CIAD, Unidad Mazatlán en Acuicultura y Manejo Ambiental, Av. Sábalo Cerritos s/n, Estero del
Yugo, C. P. 82010, A. P. 711, Mazatlán Sinaloa, México.

ABSTRACT

In this paper we present an algorithm to determine the multifocus image fusion from several color microbiological images captured from the best focusing region. This focusing region is built by including several images up and down starting from Z position of the best image in focus. The captured RGB images are converted to YCbCr color space to have the color CbCr and intensity Y channels separated with the objective to preserve the color information of the best in focus image. However this algorithm utilizes the Fourier approach by using the Y channel frequency content via analyzing the Fourier coefficients for retrieving the high frequencies in order to obtain the best possible characteristics of every captured image. After this process, we construct the fused image with these coefficients and color information for the optimum in focus image in the YCbCr color space, as a result, we obtain a precise final RGB fused image.

Keywords: fusion, Fourier transform, best focus region.

1. INTRODUCTION

An automated microscope can automatically capture and process images of a sample, where one of the goals of this process is to obtain the best sample image in which to work with. However, because microbiological organisms have volumetric structure, more than one image captured in the Z axis direction contains relevant and useful information. With these multiple images, we can construct a high quality image instead of relying on and using the best focused image.   In this context the images fusion concept emerge. The images fusion process is similar to the combination of two or more images into a single image where one retains the relevant information from each captured image[1].   There are many methods about fusion techniques. Some of them are based on wavelet transform, Laplacian, ratio, contrast or morphological pyramids selection, fusion by averaging, Bayesian methods, fuzzy sets and artificial networks[1-10]. Some applications in the past have been related with military, robotics, medical imaging, remote sensing, etc.

However, the image fusion algorithm presented in this paper is based on the Fourier transform approach.

2. MULTIFOCUS FUSION ALGORITHM BASED ON FOURIER TRANSFORM

Let us introduce some useful notation, definitions and functions: S_W is a stack of W polychromatic captured images of size NxM pixels from a biological sample taken by stepping in the microscope in the Z axis direction at Δz increments; $f_1, f_2, ..., f_K$ is a subset from S_W with K images to fuse, this subset is called the best in focus region BFR. The BFR contains the best in focus captured images and best in focus image f_{BF} obtained with an autofocus algorithm[11].   The BFR can be constructed selecting ξ quantity of images, where ξ will be the captured images selected up and down from

*josue@cicese.xm; phone +52 646 1750500; fax +52 646 175 05 53; cicese.mx/~josue

f_{BF} in the Z axis direction. Therefore, $K=2\xi+1$ images to fuse, where $K<W$ and f_{BF} will be positioned inside $f_1, f_2, ..., f_K$ with $f_{\left\lfloor \frac{K}{2} \right\rfloor +1} = f_{BF}$ where $\lfloor \tau \rfloor$ integer function of a number τ; $f^{RGB}(x,y)_k$ is the kth captured image matrix with pixels (x,y) inside *BFR,* thus $f^{RGB}(x,y)_k \in BFR \subset S_W$, where $x=1,2,...,N$, $y=1,2,...,M$ and $k=1,2,...,K$.

$f^R(x,y)_k, f^G(x,y)_k, f^B(x,y)_k$ will be the RGB decomposition channels, respectively of $f^{RGB}(x,y)_k$ with range [0, 255], where red R, green G and blue B are channels in RGB color space representation.

The equations used in this paper for the bidimensional Fourier transform are given by

$$\Im(u,v) = \int_{-\infty}^{\infty} \int_{-\infty}^{\infty} F(x,y)\, e^{-jux}\, e^{-jvy} dx\, dy\,, \tag{1}$$

$$F(x,y) = \int_{-\infty}^{\infty} \int_{-\infty}^{\infty} \Im(u,v) e^{ujx}\, e^{jvy} du\, dv\,, \tag{2}$$

where (u,v) are the spatial frequencies and $j = \sqrt{-1}$. Eq. (1) defines the bidimensional Fourier transform of $F(x,y)$. Typically, $F(x,y)$ is a function with variables in the space field and $\Im(u,v)$ is a function with variables in the spatial frequency field.

Respectively, in notational form, the Fourier transform defined in Eq. (1) can be written like operator in the following form

$$\Im(u,v) = \wp\{F(x,y)\}\,, \tag{3}$$

thus, $F(x,y)$ can be obtained by the inverse Fourier transform defined in Eq. (2) and written like operator by the expression

$$F(x,y) = \wp^{-1}\{\Im(u,v)\}\,. \tag{4}$$

2.1 Color space representation suitable to solve a fusion problem

In this paper we propose to use YCbCr color space representation because has a 16-235 nominal range when performing YCbCr to RGB conversion, this prevent to going outside 0-255 range, due video processing problem and noise generated by electronic changes, so YCbCr color space is used in this context to avoid underflow and overflow wrap-around problems[12-13].

Let us define $f^{YCbCr}(x,y)$ to be an image in the YCbCr color space representation and $f^Y(x,y), f^{Cb}(x,y)$, and $f^{Cr}(x,y)$ their respective integrating channels. The RGB to YCbCr and YCbCr to RGB color space conversions[14], can be expressed by

$$f^{YCbCr}(x,y) = \begin{bmatrix} 0.299 & 0.587 & 0.144 \\ -0.169 & -0.331 & 0.5 \\ 0.5 & -0.419 & -0.081 \end{bmatrix} \begin{bmatrix} f^R(x,y) \\ f^G(x,y) \\ f^B(x,y) \end{bmatrix}\,, \tag{5}$$

and

$$f^{RGB}(x,y) = \begin{bmatrix} 1 & -0.0009 & 1.4 \\ 1 & -0.344 & -0.714 \\ 1 & 1.772 & 0.001 \end{bmatrix} \begin{bmatrix} f^Y(x,y) \\ f^{Cb}(x,y) \\ f^{Cr}(x,y) \end{bmatrix}\,, \tag{6}$$

where $f^{YCbCr}(x,y)$ is the YCbCr color space representation of $f^{RGB}(x,y)$ y $f^{RGB}(x,y)$ is the RGB color space representation of $f^{YCbCr}(x,y)$, when $x=1,2,...,N$ and $y=1,2,...,M$. $f^{Y}(x,y)$ is the intensity or luminance channel with working range [0,255], while $f^{Cb}(x,y)$ and $f^{Cr}(x,y)$ are the color or chrominance channels with working range [-128,127]. Let us define some useful notations to represent the color space conversion defined in Eq. (5) and Eq. (6). In this sense, $\Phi^{YCbCr}\{f^{RGB}(x,y)\}$ is defined to be the conversion $RGB \rightarrow YCbCr$ image function expressed in notational form by

$$f^{YCbCr}(x,y) = \Phi^{YCbCr}\{f^{RGB}(x,y)\}, \tag{7}$$

while, $\Phi^{RGB}\{f^{YCbCr}(x,y)\}$ is defined to be the conversion $YCbCr \rightarrow RGB$ image function written in notational form by

$$f^{RGB}(x,y) = \Phi^{RGB}\{f^{YCbCr}(x,y)\}, \tag{8}$$

2.2 Multifocus fusion algorithm

At the present, several fusion techniques are based in alternative techniques, i.e. Wavelets, ratio, average, pyramids, etc. Fourier transform is a robust tool highly proved during several decades and never has been used, to our knowledge, for image fusion algorithms develop. FFT give us a high sensible analysis of frequency coefficients from the images involved in the fusion algorithm than DCT, and with FFT, the final fused image is constructed with higher definition.

Let us obtain $f_{BF}^{YCbCr}(x,y) = \Phi^{YCbCr}\{f_{BF}\}$ where $f_{BF}^{YCbCr}(x,y)$ is the best image in focus transformed in YCbCr color space representation and their respective $f_{BF}^{Y}(x,y), f_{BF}^{Cb}(x,y)$ and $f_{BF}^{Cr}(x,y)$ YCbCr integrated channels. After obtaining $f_{BF}^{YCbCr}(x,y)$, we continue getting the YCbCr color space representation of $f_1, f_2,..., f_K$ images by the expression

$$f^{YCbCr}(x,y)_k = \Phi^{YCbCr}\{f(x,y)_k\} \quad \text{for} \quad k=1,2,...,K. \tag{9}$$

Once, we have $f_1, f_2,..., f_K$ images transformed to YCbCr color space representation according Eq. (9), we obtain their respective $f^{Y}(x,y)_k$, $f^{Cb}(x,y)_k$ and $f^{Cr}(x,y)_k$ YCbCr integrated channels.

The final fused image $f^{RGB*}(x,y)$ can be obtained by

$$f^{RGB*}(x,y) = \Phi^{RGB}\{f^{YCbCr*}(x,y)\}, \tag{10}$$

where $f^{YCbCr*}(x,y)$ is the fused image in YCbCr color space representation, thus $f^{YCbCr*}(x,y)$ can be obtained by

$$f^{YCbCr*}(x,y) = \{f^{Y*}(x,y) \cup f_{BF}^{Cb}(x,y) \cup f_{BF}^{Cr}(x,y)\} \tag{11}$$

thus $f^{YCbCr*}(x,y)$ is the result of constructing a tri-dimensional matrix by the union of the $f^{Y*}(x,y), f_{BF}^{Cb}(x,y)$ and $f_{BF}^{Cr}(x,y)$ channels. In this context, $f^{Y*}(x,y)$ is the fused Y channel obtained by the magnitude of inverse Fourier transform of the fused Y channel Fourier transform $f^{Y**}(u,v)$, then $f^{Y*}(x,y)$ can be acquired by

$$f^{Y*}(x,y) = \left| \wp^{-1}\{f^{Y**}(u,v)\} \right|. \tag{12}$$

Let $f^{Y***}(u,v)_k = \wp\{f^{Y}(x,y)_k\}$ be the Fourier transform of Y channel of the kth image inside *BFR*. Therefore, $f^{Y**}(u,v)$ can be obtained by the following expression

$$f^{Y**}(u,v) = \begin{cases} f^{Y***}(u,v)_k & if \quad \left|f^{Y***}(u,v)_k\right| \geq \left|f^{Y***}(u,v)_{k+1}\right| \\ f^{Y***}(u,v)_{k+1} & otherwise \end{cases}, \tag{13}$$

for $u=1,2,..., N$, $v=1,2,..., M$, $k=1,2,..., K$-1 and $\left|f^{Y***}(u,v)_k\right|$ is the Fourier magnitude of Y channel of the kth image. Ultimately, Eq. (13) defines the proposed algorithm kernel where the best characteristics of every image to be fused

remains in $f^{Y**}(u,v)$ after the process. Finally we used the f_{BF} color information to obtain the final fused image $f^{RGB*}(x,y)$. However, this algorithm analyzes all coefficients from the images where the highest energy is concentrated in two or four coefficients which are in the low frequency region only. But, the remaining coefficients, which have information of the high frequencies, represent the best visual characteristics of the images. For this reason, when we obtain the maximum of the magnitude of the Fourier coefficient from the images to be fused, the low frequencies have no effect on the resulting fused image.

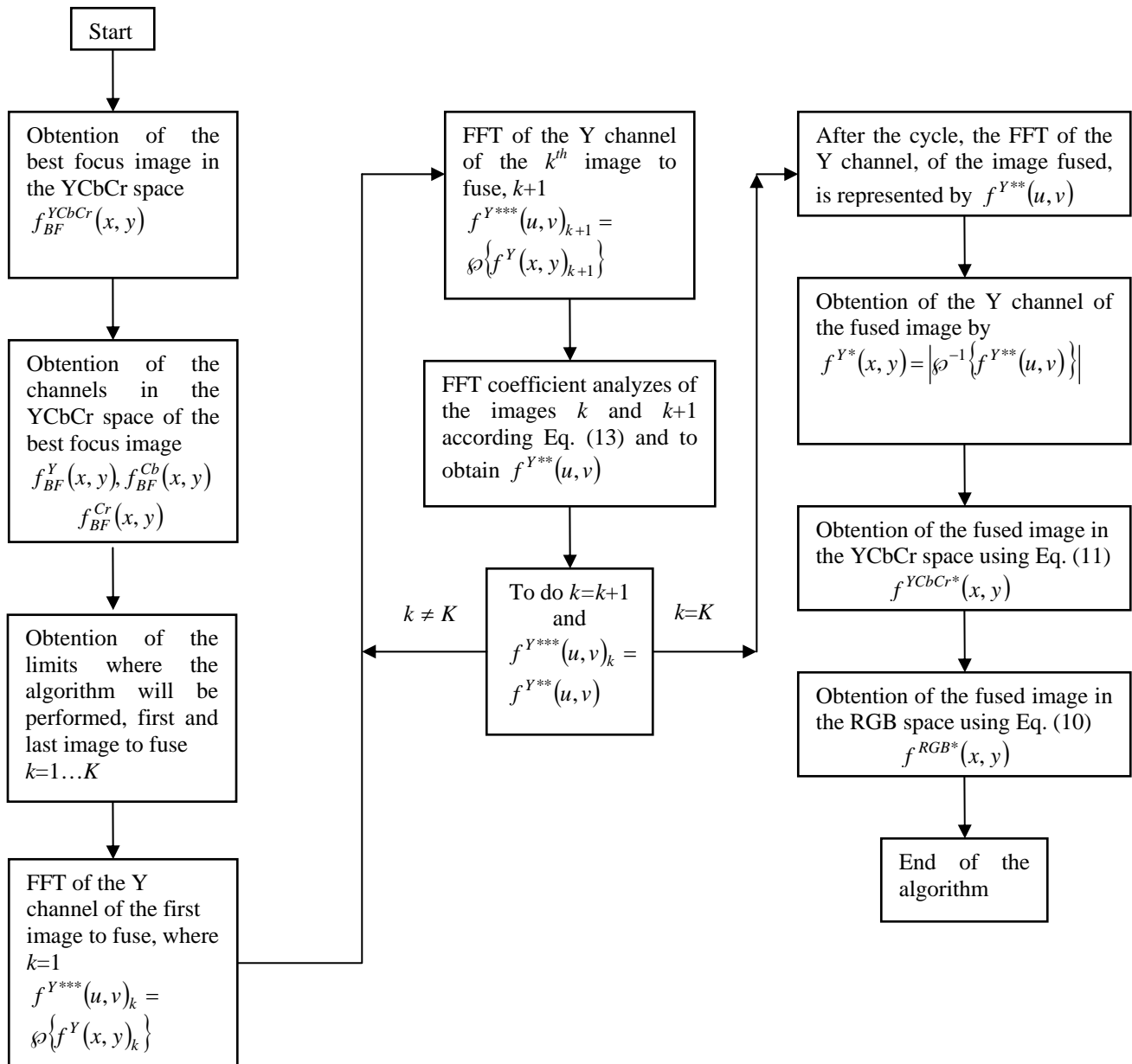Fig. 1 shows in blocks the algorithm used.

Start

Obtention of the best focus image in the YCbCr space
$f_{BF}^{YCbCr}(x,y)$

Obtention of the channels in the YCbCr space of the best focus image
$f_{BF}^{Y}(x,y), f_{BF}^{Cb}(x,y)$
$f_{BF}^{Cr}(x,y)$

Obtention of the limits where the algorithm will be performed, first and last image to fuse
$k=1\ldots K$

FFT of the Y channel of the first image to fuse, where $k=1$
$f^{Y***}(u,v)_k = \wp\{f^{Y}(x,y)_k\}$

FFT of the Y channel of the kth image to fuse, $k+1$
$f^{Y***}(u,v)_{k+1} = \wp\{f^{Y}(x,y)_{k+1}\}$

FFT coefficient analyzes of the images k and $k+1$ according Eq. (13) and to obtain $f^{Y**}(u,v)$

$k \neq K$

To do $k=k+1$ and
$f^{Y***}(u,v)_k = f^{Y**}(u,v)$

$k=K$

After the cycle, the FFT of the Y channel, of the image fused, is represented by $f^{Y**}(u,v)$

Obtention of the Y channel of the fused image by
$f^{Y*}(x,y) = |\wp^{-1}\{f^{Y**}(u,v)\}|$

Obtention of the fused image in the YCbCr space using Eq. (11)
$f^{YCbCr*}(x,y)$

Obtention of the fused image in the RGB space using Eq. (10)
$f^{RGB*}(x,y)$

End of the algorithm

Figure 1: Algorithm fusion flow diagram.

3. Results

Two hundred twenty images integrating an image stack were captured from a microscope to test the fusion properties of the proposed algorithm for a shrimp tissue sample where it is possible to find inclusion bodies of virus. These images were taken with a Z increment of 0.1 μm. The images were taken form a real sample utilizing a digital color CCD camera from LEICA (model DC 300). The camera connected directly to a LEICA DMRXA2 microscope; on the other hand, the resolution used to take these images was 2088 x 1550 pixels and were captured without any previous image correctness process. The equipment used was a 2.5 GHz PC Pentium 4 with 1 GByte RAM and 80 GBytes HD.

After the image stack was captured, it was processed by an autofocus algorithm[11] to obtain the best image on focus. After the focused image was obtained, we selected the images to be fused. The selected images will shape the best focus region, *BFR*, where the fusion process will be applied. Figure 2a shows the best image on focus made by an autofocus algorithm[11] and Fig. 2b shows the image fused by the algorithm presented in this paper. You can see the difference between both (Figs. 2c and 2d). The images represents the microscopical image of a shrimp tissue sample. These images have three dimensional information.
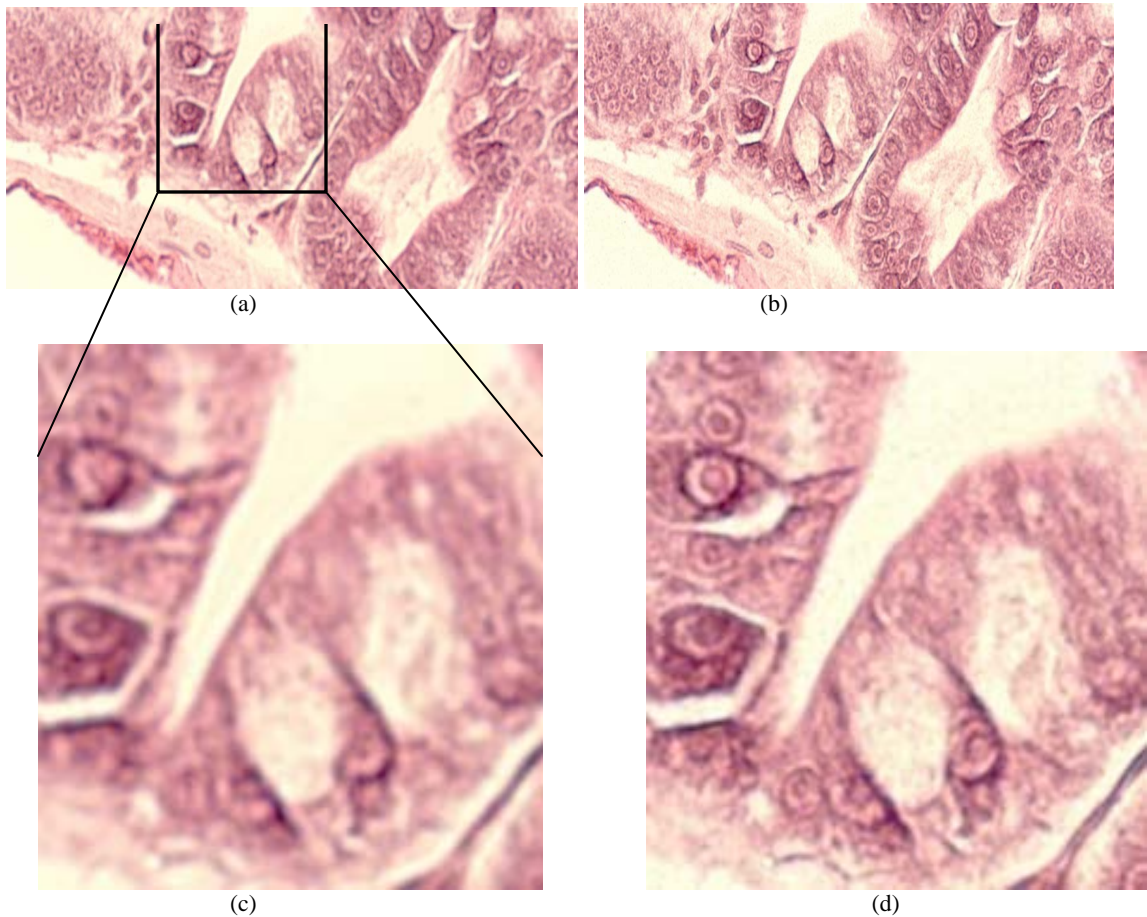

(a)   (b)

(c)   (d)

Figure 2: Images of a shrimp tissue sample

(a)   (b)

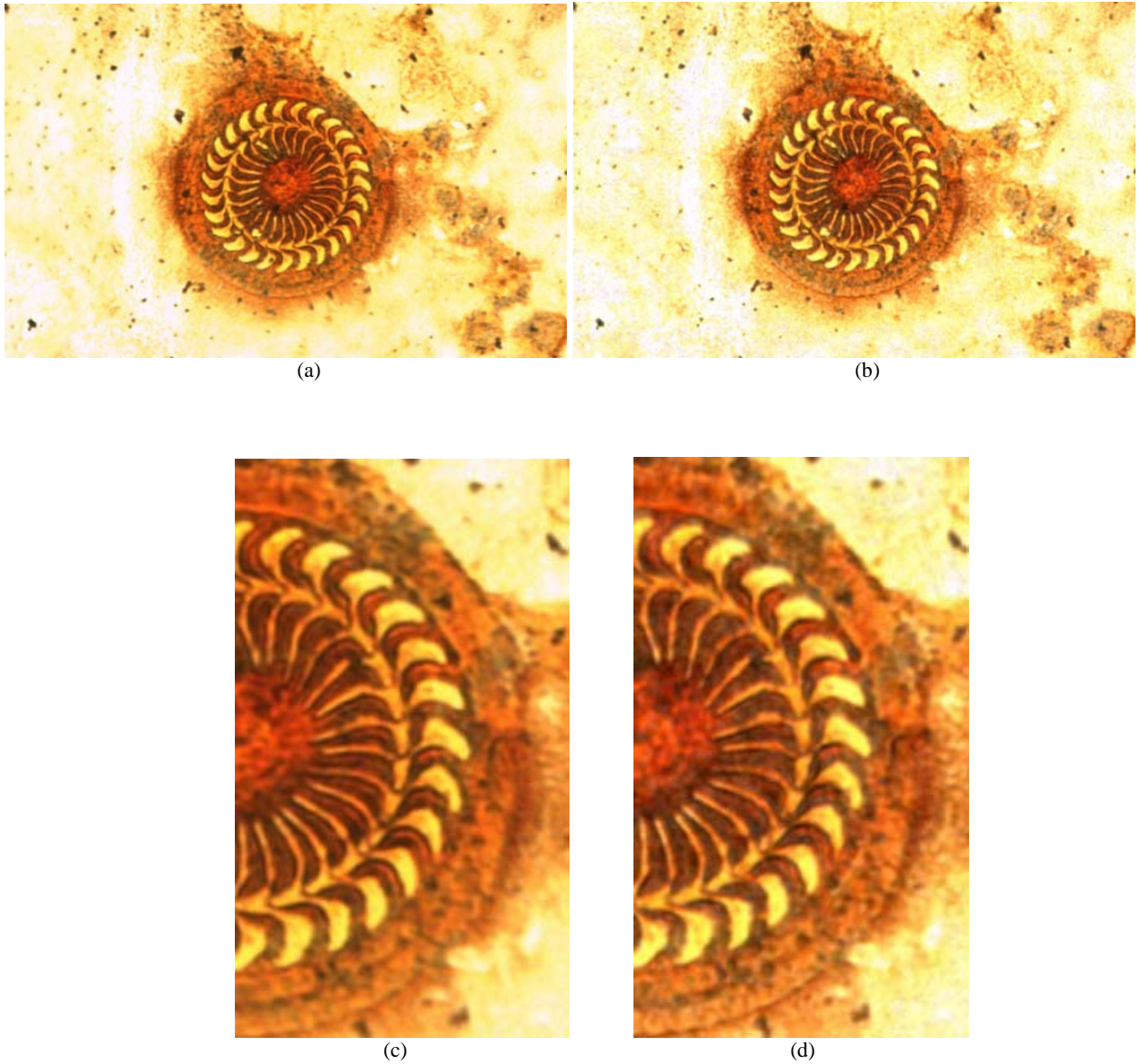(c)   (d)

Figure 3: Images of a Trichodine.

Eighty images integrating an image stack were captured from a microscope to test the fusion properties of the proposed algorithm for a biological microorganism from the genus Trichodine, a protozoan fish parasite. These images were taken with a Z increment of 0.5 μm. Figure 3a shows the best image on focus made by an autofocus algorithm[11] and Fig. 3b shows the image fused by the algorithm presented in this paper. You can see the difference between both (Figs. 3c and 3d). These images have three dimensional information.   In this case the difference is not so big because almost all the information is in the same plane and the increment in Z was bigger compared with the first example.

4. Conclusions

In this paper a new fusion method for color images has been presented. This new algorithm offers a significant performance when several images are needed to be interpreted with visual high quality. Thus, the proposed algorithm

will be suitable for implementation in real-time processing. This is due to the algorithm's robustness and accuracy in fusing several types of real images obtained from different kinds of samples.

Acknowledgments

REFERENCES

1. Hill Paul, Canagarajah Nishan and Bull Dave, "Image Fusion using Complex Wavelets", British Machine Vision Conference, Book BMCV02, Sep. (2002).

2. Zheng Yufeng, Essock Edward A. and Hansen Bruce C., "An advanced image fusion algorithm based on wavelet transform: incorporation with PCA and morphological processing", Image Processing, Proc. SPIE Vol. 5298, pp. 177-187, May. (2004).

3. Forero Manuel G., Sroubek Filip, Flusser Jan, Redondo Rafael and Cristóbal Gabriel, "Automatic screening and multifocus fusion methods for diatom identification", Applications and Science of Neural networks, Fuzzy Systems and Evolutionary Computation VI, Proc. SPIE Vol. 5200, pp. 197-206, Dec. (2003).

4. Rockinger, O., "Pixel level fusion of image sequences using wavelet frames", Proc. 16th Leeds Annual Statistical Research Workshop, Leeds University Press, pp. 149-154, (1996).

5. Bloch I., Maitre Henri "Data fusion in 2D and 3D image processing: an overview", Graphics and Image Processing, SIBGRAPI, Campos do Jordao, Brazil, pp. 127-134, (1997).

6. Bloch I., Maitre Henri, "Image Fusion", International Science Foundation Workshop on Data Mining, Granada (Spain), Apr. (1997).

7. Sharma Ravi K. and Pavel Misha, "Adaptive and statistical image fusion", Society for Information Display Digest, Vol. XXVII, pp. 969-972, May. (1996).

8. Li Shutao, Kwok James T. and Wang Yaonan, "Multifocus image fusion using artificial neural", Pattern Recognition Letters, Vol. 23(8), pp. 985-997, Jun. (2002).

9. Petrovic Vladimir, "Multilevel image fusion", Proc. SPIE Vol. 5099, pp. 87-96, Apr. (2003).

10. Achalakul Tiranee, Haaland Peter D., Taylor Stephen, "Math Web: a concurrent image analysis tool suite for multispectral data fusion", Proc. SPIE Vol. 3719, pp. 351-358, Mar. (1999).

11. Bueno Mario A., Alvarez-Borrego Josué, Acho Leonardo, Chávez-Sánchez María Cristina, "Fast Autofocus Algorithm for Automated Microscopes", Optical Engineering, Vol. 44, No. 6, June (2005).

12. ITU-R BT.601–5, 1995, Studio Encoding Parameters of Digital Television for Standard 4:3 and Widescreen 16:9 Aspect Ratios.

13. Devereux, V. G., 1987, Limiting of YUV digital video signals, BBC Research Department Report BC RD1987 22.

14. Pratt William K., "Digital image processing", 2nd Edition, Wiley Interscience Press, USA, pp. 62-72, (1991).

Fusion Algorithm For Color Microbiological Organisms Images In Automatized Microscopes

Josué Álvarez-Borrego[1], Mario Alonso Bueno-Ibarra[1,5], Vitaly Kober[2], Cristian Gallardo-Escárate[1,3], Maria C. Chávez-Sánchez[4], Emma Fájer-Ávila[4]

[1]Dirección de Telemática, [2]Departamento de Ciencias Computacionales. Centro de Investigación Científica y de Educación Superior de Ensenada. Km 107 Carretera Tijuana- Ensenada, Código Postal 22860. Ensenada, B.C. México. [3]Departamento de Biología Marina, Facultad de Ciencias del Mar, Universidad Católica del Norte. Larrondo 1281, Casilla 117, Coquimbo. Chile. [4]CIAD, Unidad Mazatlán en Acuicultura y Manejo Ambiental, Av. Sábalo Cerritos s/n, Estero del Yugo, C. P. 82010, A. P. 711, Mazatlán Sinaloa, México. [5]Universidad Autónoma de Ciudad Juárez, Instituto de Ingeniería y Tecnología, Departamento de Ingeniería Eléctrica y Computación, Av. Del Charro 450 Norte, C. P. 32310, Ciudad Juárez, Chih., México.

ABSTRACT

In this paper we present an algorithm to determine the multifocus image fusion from several color microbiological images captured from the best focusing region. This focusing region is built by including several images up and down starting from Z position of the best image in focus. The captured RGB images are converted to YCbCr color space to have the color CbCr and intensity Y channels separated with the objective to preserve the color information of the best in focus image. However this algorithm utilizes the Fourier approach by using the Y channel frequency content via analyzing the Fourier coefficients for retrieving the high frequencies in order to obtain the best possible characteristics of every captured image. After this process, we construct the fused image with these coefficients and color information for the optimum in focus image in the YCbCr color space, as a result, we obtain a precise final RGB fused image.

INTRODUCTION

An automated microscope can automatically capture and process images of a sample, where one of the goals of this process is to obtain the best sample image in which to work with. However, because microbiological organisms have volumetric structure, more than one image captured in the Z axis direction contains relevant and useful information. With these multiple images, we can construct a high quality image instead of relying on and using the best focused image. In this context the images fusion concept emerge. The images fusion process is similar to the combination of two or more images into a single image where one retains the relevant information from each captured image[1]. There are many methods about fusion techniques. Some of them are based on wavelet transform, Laplacian, ratio, contrast or morphological pyramids selection, fusion by averaging, Bayesian methods, fuzzy sets and artificial networks[1-10].
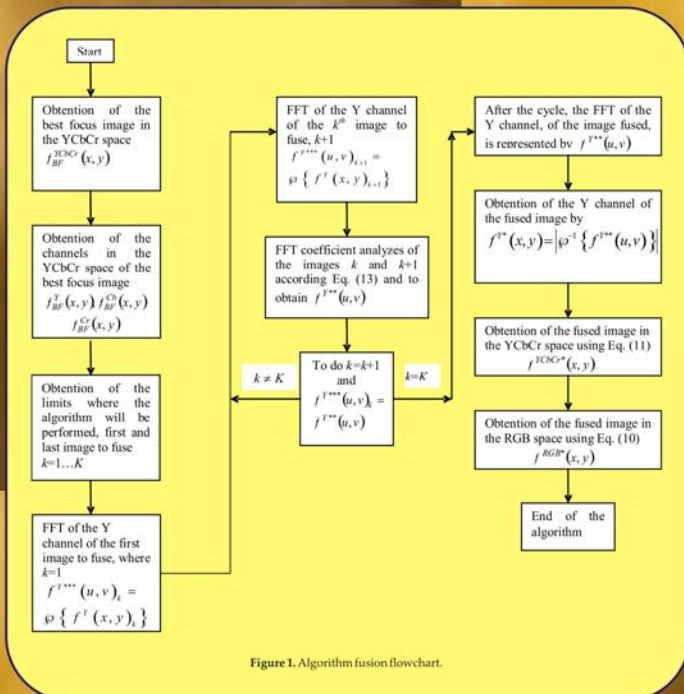
MULTIFOCUS FUSION ALGORITHM

Figure 1. Algorithm fusion flowchart.

$$f^{RGB*}(x,y)=\Phi^{RGB}\left\{f^{YCbCr*}(x,y)\right\}, \quad (10)$$

$$f^{YCbCr*}(x,y)=\left\{f^{Y*}(x,y)\cup f^{Cb}_{BF}(x,y)\cup f^{Cr}_{BF}(x,y)\right\} \quad (11)$$

$$f^{Y*}(x,y)=\left|\wp^{-1}\left\{f^{Y**}(u,v)\right\}\right|. \quad (12)$$

$$f^{Y**}(u,v)=\begin{cases} f^{Y***}(u,v)_k & \text{if } \left|f^{Y***}(u,v)_k\right|\geq\left|f^{Y***}(u,v)_{k+1}\right| \\ f^{Y***}(u,v)_{k+1} & \text{otherwise} \end{cases}. \quad (13)$$

Figure 2. Additional algorithm equations.

RESULTS

Two hundred twenty images integrating an image stack were captured from a microscope to test the fusion properties of the proposed algorithm for a shrimp tissue sample where it is possible to find inclusion bodies of virus. These images were taken with a Z increment of 0.1 μm. The images were taken form a real sample utilizing a digital color CCD camera from LEICA (model DC 300). The camera connected directly to a LEICA DMRXA2 microscope; on the other hand, the resolution used to take these images was 2088 x 1550 pixels and were captured without any previous image correctness process. The equipment used was a 2.5 GHz PC Pentium 4 with 1 GByte RAM and 80 GBytes HD.

After the image stack was captured, it was processed by an autofocus algorithm[11] to obtain the best image on focus. After the focused image was obtained, we selected the images to be fused. The selected images will shape the best focus region, *BFR*, where the fusion process will be applied. Figure 3a shows the best image on focus made by an autofocus algorithm[11] and Fig. 3b shows the image fused by the algorithm presented in this paper. You can see the difference between both (Figs. 3c and 3d). The images represents the microscopical image of a shrimp tissue sample. These images have three dimensional information.
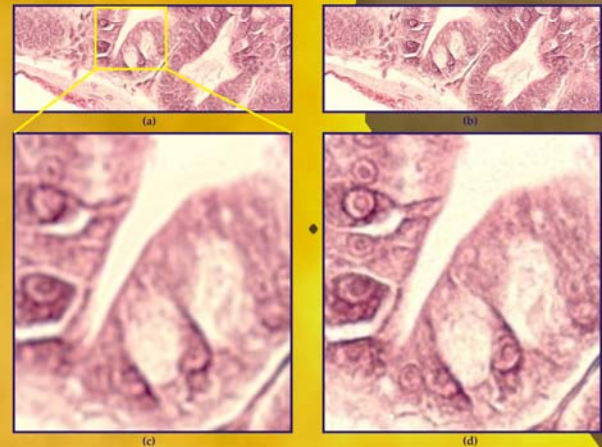

Figure 3. Images of shrimp tissue sample.

CONCLUSIONS

In this paper a new fusion method for color images has been presented. This new algorithm offers a significant performance when several images are needed to be interpreted with visual high quality. Thus, the proposed algorithm will be suitable for implementation in real-time processing. This is due to the algorithm's robustness and accuracy in fusing several types of real images obtained from different kinds of samples.

REFERENCES

1. Hill Paul, Canagarajah Nishan and Bull Dave, "Image Fusion using Complex Wavelets", British Machine Vision Conference, Book BMCV02, Sep. (2002).

2. Zhang Yufeng, Essock Edward A. and Hansen Bruce C., "An advanced image fusion algorithm based on wavelet transform: incorporation with PCA and morphological processing", Image Processing, Proc. SPIE Vol. 5298, pp. 177-187, May. (2004).

3. Forero Manuel G., Sroubek Filip, Flusser Jan, Redondo Rafael and Cristóbal Gabriel, "Automatic screening and multifocus fusion methods for diatom identification", Applications and Science of Neural networks, Fuzzy Systems and Evolutionary Computation VI, Proc. SPIE Vol. 5200, pp. 197-206, Dec. (2003).

4. Rockinger, O., "Pixel level fusion of image sequences using wavelet frames", Proc. 16th Leeds Annual Statistical Research Workshop, Leeds University Press, pp. 149-154, (1996).

5. Bloch I., Maitre Henri "Data fusion in 2D and 3D image processing: an overview", Graphics and Image Processing, SIDGRAPI, Campos do Jordao, Brazil, pp. 127-134, (1997).

6. Bloch I., Maitre Henri, "Image Fusion", International Science Foundation Workshop on Data Mining, Granada (Spain), Apr. (1997).

7. Sharma Ravi K. and Pavel Misha, "Adaptive and statistical image fusion", Society for Information Display Digest, Vol. XXVII, pp. 969-972, May. (1996).

8. Li Shutao, Kwok James T. and Wang Yaonan, "Multifocus image fusion using artificial neural", Pattern Recognition Letters, Vol. 23(8), pp. 985-997, Jun. (2002).

9. Petrovic Vladimir, "Multilevel image fusion", Proc. SPIE Vol. 5099, pp. 87-96, Apr. (2003).

10. Achalakul Tiranee, Haaland Peter D., Taylor Stephen, "MuSE Web: a concurrent image analysis tool suite for multispectral data fusion", Proc. SPIE Vol. 3719, pp. 351-358, Mar. (1999).

11. Bueno Mario A., Alvarez-Borrego Josué, Acho Leonardo, Chávez-Sánchez Maria Cristina, "Fast Autofocus Algorithm for Automated Microscopes", Optical Engineering, Vol. 44, No. 6, June (2005).

12. ITU-R BT.601-5, 1995, Studio Encoding Parameters of Digital Television for Standard 4:3 and Widescreen 16:9 Aspect Ratio.

13. Devereux, V. G., 1987, Limiting of YUV digital video signals, BBC Research Department Report BC RD1987 22.

14. Pratt William K., "Digital image processing", 2nd Edition, Wiley Interscience Press, USA, pp. 62-72, (1991).